A R C H I V E S O F M E T A L L U R G Y A N D M A T E R I A L S
Volume 54 2009 Issue 3

P. SZOTA*, A. STEFANIK*, H. DYJA*

ANALYSIS OF BIMETALLIC BAR ROLLING PROCESS IN THREE-SKEW ROLLING MILL

NUMERYCZNA ANALIZA PROCESU WALCOWANIA PRĘTÓW BIMETALOWYCH W TRÓJWALCOWEJ WALCARCE SKOŚNEJ

Production of the reinforcement bimetallic bars steel – corrosion resistant steel is very difficult and there are many theological problems of this process. The main difficult during production of the bimetallic bars is production of the bimetallic stock, which have to characterized adequate strange joining between core and platter layer and a uniformly thickness of platter layer on the round and length of stock. To the production of the bimetallic stock the three – skew rolling process could be used.

Applies of the three-skew rolling mill to the production of the bimetallic stock could provide to obtain a good quality bimetallic bars without lapping of platter layer on the bar cross-section and with adequate strength joining between bimetallic bar components. The three – skew rolling process allows application of the height deformation of the stock in a single pass.

A theoretical analysis of bimetallic bar rolling in the three-skew rolling mill was presented in this paper. The distributions of stress and strain intensities, temperature and strain rate in the bimetallic bar during skew rolling are shown. The simulations of the bar rolling in a three-skew rolling mill were carried out using the Forge2005® commercial program.

Keywords: hot rolling process, three-skew rolling mill, fem, bimetallic bar

Wytwarzanie bimetalowych prętów żebrowanych stal – stal odporna na korozję jest procesem bardzo złożonym i wiąże się z wieloma problemami technologicznymi. Trudności podczas wytwarzania takich prętów związane są ze sposobem otrzymania wsadu bimetalowego, który cechowałby się odpowiednią wytrzymałością połączenia warstwy platerującej i rdzenia oraz równomierną grubością warstwy platerującej na obwodzie i długości rdzenia. Do otrzymania wsadu bimetalowego można wykorzystać metodę walcowania w trójwalcowej walcarce skośnej.

Zastosowanie trójwalcowej walcarki skośnej może zapewnić uzyskiwanie dobrego jakościowo wsadu bimetalowego, bez zawalcowania warstwy platerującej na przekroju poprzecznym pręta oraz z dobrym połączeniem poszczególnych warstw bimetalowego pręta. Cechą charakterystyczną procesu walcowania prętów w trójwalcowych walcarkach skośnych jest możliwość stosowania dużych odkształceń w jednym przepuście.

W ramach badań przeprowadzono analizę teoretyczną procesu walcowania w trójwalcowej walcarce skośnej na podstawie, której określono wpływ charakterystycznych parametrów na proces walcowania. Modelowanie numeryczne procesu walcowania wykonano z wykorzystaniem programu komputerowego Forge2005®.

1. Introduction

A considerable increase in interest in using corrosion resistant steel clad ribbed bars in the construction industry has been observed in recent years. This is owing to the particular properties of these bars, namely high durability and rigidity, good mechanical properties, and high corrosion resistance.

An analysis of the durability and strength of iron-concrete structures carried out at the University of Kansas Center for Research, the USA, shows that the use of bimetallic ribbed bars yields considerable savings during the long-term operation of those structures [1]. A problem encountered in the production of such bars is to develop a technology for the production of bimetallic feedstock.

Different methods are used for producing bimetallic feedstock in the form of round bars designed for further plastic working. One of the methods of manufacturing bimetallic feedstock is rolling of bimetallic bar components on a three-skew rolling mill (Fig. 1). The advantage of rolling on the three-skew rolling mill is

* CZĘSTOCHOWA UNIVERSITY OF TECHNOLOGY, FACULTY OF MATERIAL PROCESSING TECHNOLOGY AND APPLIED PHYSICS, INSTITUTE OF MODELLING AND AUTOMATION OF PLASTIC WORKING PROCESSES, UL. ARMII KRAJOWEJ 19, 42-200 CZĘSTOCHOWA, POLAND

the occurrence of a difference between peripheral speeds along the deformation zone. Increasing the roll diameter in the direction of the exit plane results in an increase in peripheral speed in the sample and the cladding layer gripping on the core. Owing to this, it is possible to obtain a fixed bond between the bimetal components.

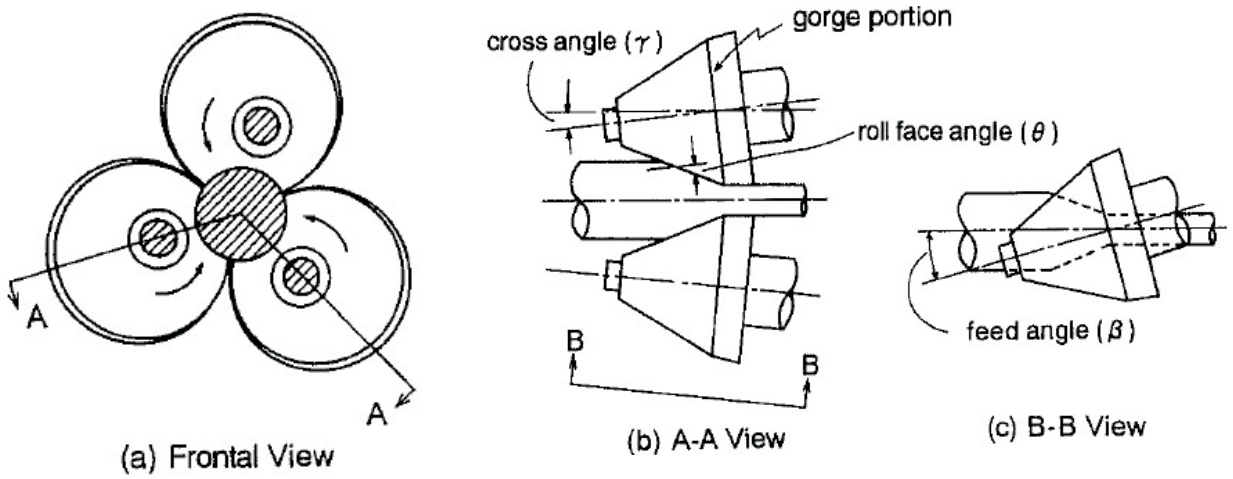

Fig. 1. Scheme of round bimetallic bar rolling process [2]

The production of steel-corrosion resistant steel bimetallic ribbed bars is a complex process and is associated with many engineering problems. The most important of them include the need to obtain bimetallic feedstock with the adequate strength of bond in the region of contact between the core and the cladding layer, and to assure the uniform plastic flow of both bimetal layers during the course of the rolling process. Failure to meet these conditions may cause a delamination of the bimetallic sample being rolled or the occurrence of other defects. An incorrect selection of the scheme of bimetallic sample deformation in the three-skew rolling mill may be the cause of the cladding layer "flowing down" from the core surface and a complex strain state which, in turn, can cause the formation of defects (such as an uneven layer thickness, microcracks, delaminations, etc.) in the cladding layer [3-5]. A correctly designed rolling process should assure a uniform and correctly thick cladding layer over both the perimeter and the length of the bar, which will not break in a subsequent process, e.g. continuous rolling into finished bimetallic ribbed bar.

The purpose of the undertaken theoretical studies is to determine the effect of the roll diameter and roll rotational speed on the process of rolling on the three-skew rolling mill and on the strain and stress state within the roll gap.

2. Numerical modelling of rolling process in three-skew rolling mill

The thermomechanical simulation of the bimetallic bars in the three-skew rolling mill rolling process was carried out using the visco-plastic body model for a three-dimensional strain state with the use of the Forge2005® program. Deformation of the body was described by the Norton-Hoff law [6].

Computer simulation of the rolling process run on the three-skew rolling mill is illustrated schematically in Figure 2. Figure 2a shows the design of roll arrangement, and the positioning of the bimetallic feedstock and the centring tool. The rolls are positioned obliquely to the rolling axis, at an angle of α=18°. The roll working surfaces are inclined at an angle of β=9° in relation to the roll axis. Such a positioning of the rolls in relation to each other enabled a 20 mm-diameter bar to be rolled out. The shape and dimensions of the rolls are shown in Figure 2b, while the dimensions statement of roll design is given in Table 1. Moreover, Fig. 2c shows a bimetallic feedstock composed of a C45 steel bar and a 306L steel tube constituting a cladding layer. The diameter of the round bar was d2=31.8 mm, while the tube outer diameter was d1=38 mm. The outer layer accounted for 30 percent of the overall area of the bimetallic feedstock cross-section.

A centring tool was added in simulation, which was intended to keep the sample end in the rolling axis and guide it stably into the deformation zone.

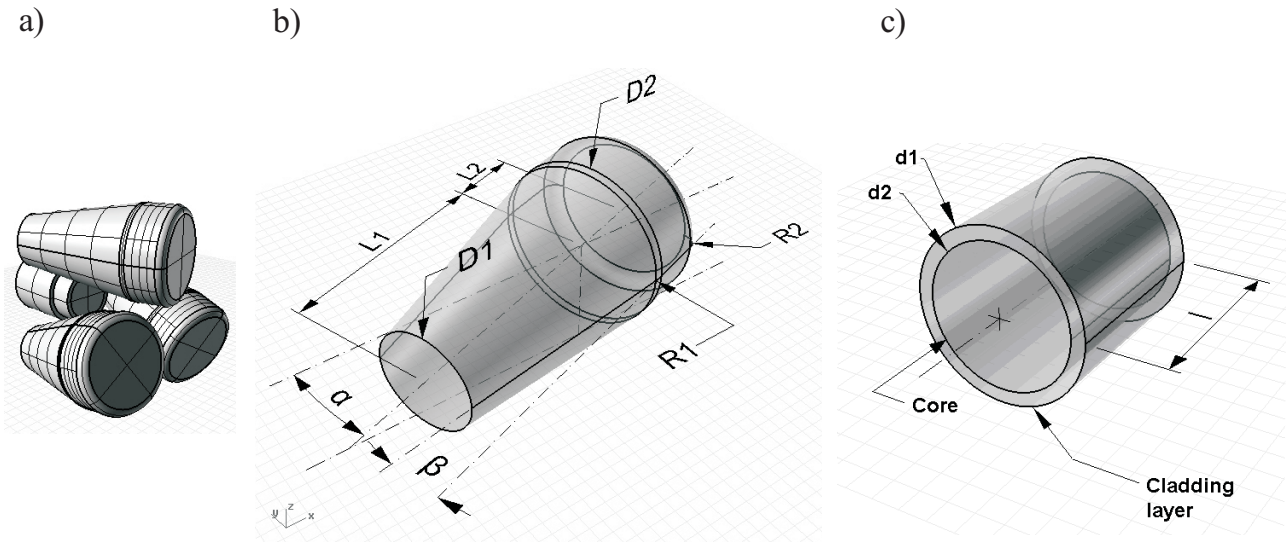

Fig. 2. Shape of the object used in numerical modeling: a) position of rolls, b) roll dimensions, c) bimetallic bar dimensions

TABLE 1

Roll dimensions used in theoretical analysis

Simulation variant	Working part diameter D1 [mm]	Calibrated part diameter D2 [mm]	Roll rotational speed ω [rpm]	Roll inclination angle β [°]	Inclination angle of axis roll α [°]	Working part length L1 [mm]	Calibrated part length L2 [mm]
I	34,7	60	100	9	18	80	25
II	57,1	100	100	9	18	80	25
III	34,7	60	200	9	18	80	25

The models of the objects shown in Figure 2 were developed in a CAD-type program, and on their basis a spatial finite-element grid was generated in the Forge2005® program. The nodes of the finite-element grids for the core and the cladding layer (bimetallic feedstock) were not shared. The connection between those elements was defined as rigidly adhering.

Simulation of the three-skew rolling mill rolling process was conducted with the following initial parameters: bimetallic feedstock temperature 1000°C (a uniform temperature distribution was assumed); rolls rotational speeds: 100 rpm and 200 rpm, rolls diameters: 60 mm and 100 mm; and the friction factor 0.8. The coefficient of heat transfer between the sample and the rolls was assumed to be 3000 W/(K·m^2) and was taken from the Forge2005® program's database. The coefficient of heat transfer between the core and the cladding layer was assumed at 60000 (W/K·m^2), as determined by the reverse method based on the distribution of temperature within an homogeneous bar being cooled.

The bimetallic feedstock was rolled in a single pass into a bimetallic bar of a final diameter of 20 mm according to three variants that differed in the rolls diameter and rolls rotational speed. Data for rolling according to the three variants is given in Table 1.

A key element of numerical modelling is defining the properties of steel in the computer program. This is especially important when a bimetal is to be rolled and the properties of the two metals are different. Therefore, it is necessary to perform the analysis of those properties.

Figure 3 shows graphically the rheological properties of two steel grades for a strain rate of 10 s^{-1}. When analyzing the graphs in Fig. 3, a clear effect of deformation and temperature can be found. Also, the strain rate has a great influence on the yield stress magnitude. By comparing the graphs in both figures it can be stated that the yield stress values for steel 306L are much greater than for steel C45. This difference has a considerable influence on the process of rolling bimetallic bar. Higher yield stress values for steel 306L, or the cladding layer, provide conditions favourable both to the production of bimetallic feedstock by the method of rolling on the three-skew rolling mill, and to further forming of the bimetallic bar in shape passes into finished bimetallic ribbed bar.

a)

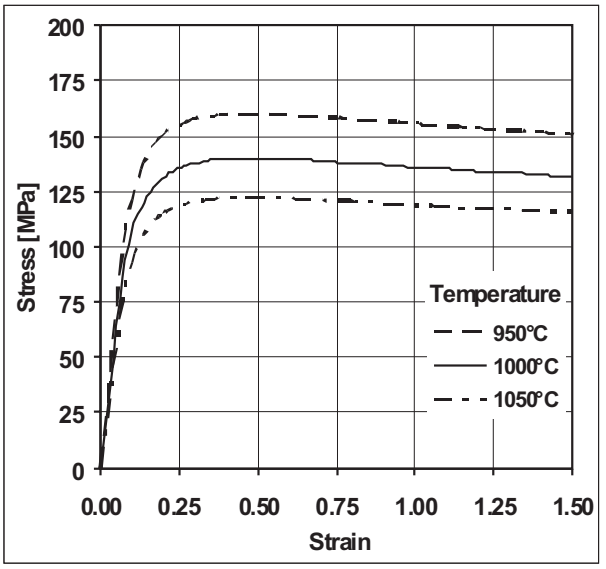

b)

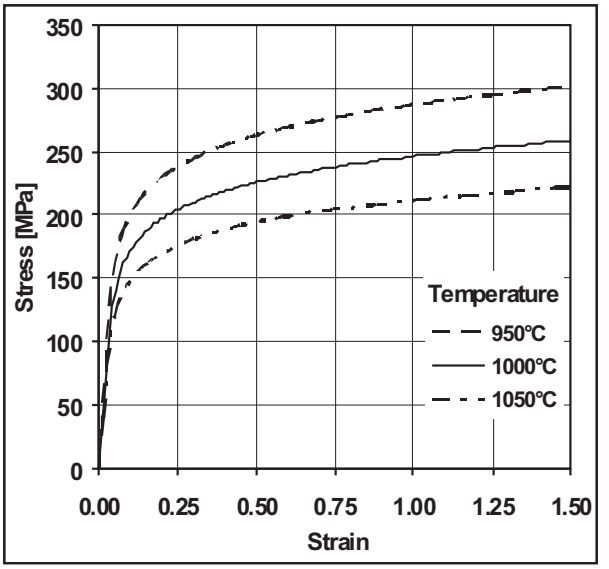

Fig. 3. Rheological properties: a) steel C45, b) steel 306L

The increased deformation resistance of the cladding layer compared to the bar core reduces the cladding layer "flow-down" effect. However, during rolling in the finishing ribbed pass, increased yield stress values being also the result of cladding layer cooling, in some instances can cause the formation of cracks in the cladding layer [1,4].

The properties of steels C45 and 306L shown in Figure 3 were entered in the program using the Henzel-Spitel function (1).

$$\sigma_p = A_0 e^{m_1 T} \varepsilon^{m_2} \dot{\varepsilon}^{m_3} e^{\frac{m_4}{\varepsilon}} \tag{1}$$

where: T – temperature, ε – strain, $\dot{\varepsilon}$ – strain rate, values of coefficients A_0, m_1-m_4 for both steel. The coefficients are taken from the material database of the program Forge2005® (Table 2).

TABLE 2

Parameters of steels properties

Steel	A_0	m_1	m_2	m_3	m_4
C45	1521.3	- 0.00269	- 0.12651	0.14542	- 0.05957
306L	4321.6	- 0.00305	0.10835	0.08647	- 0.01270

3. Research results

As the result of numerical studies carried out according to Variants I, II and III (Table 1), bimetallic bars of similar dimensions were obtained. Selected example of calculated shape of the sample during rolling is presented on Figure 4a. The shape and dimensions of the obtained bimetallic bar are shown in Figure 4b. The dark areas on the surface of the rolled sample (Fig. 4a) indicate the locations of contact between the sample and the rolls, as well as the locations of sample contact with the centring tool.

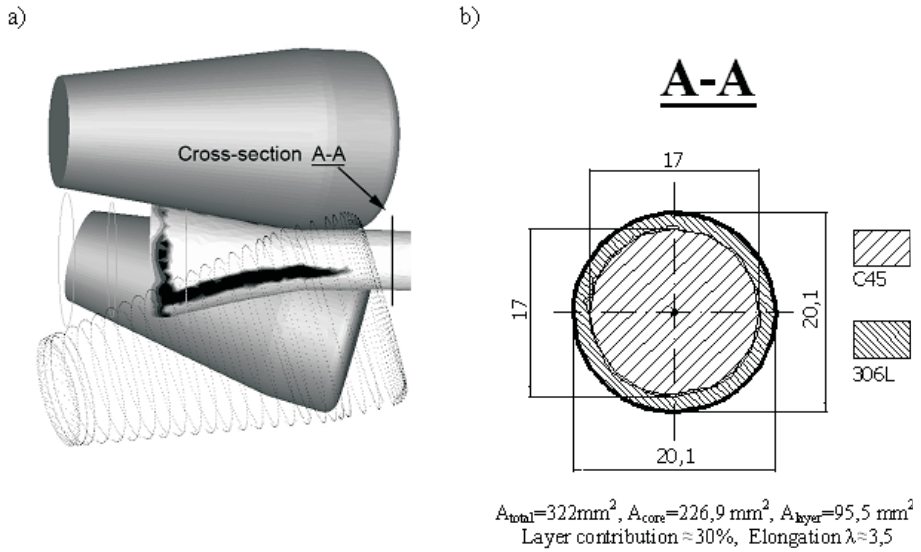

Fig. 4. Results of the numerical modeling: a) shape of bimetallic bar, b) dimensions of the bimetallic bar on cross-section

The obtained dimensions of the bimetallic bar on its cross-section were achieved immediately after the bar had exited the deformation zone (after the roll sizing zone, the cross-section A-A). During rolling, the grid surfaces at the contact between the core and the cladding layer were distorted as a result of the occurrence of a large deformation and twisting moments. This creates a difficulty in determining the inner diameter of the bimetallic bar. Therefore, the theoretical diameter, as calculated from the surface area of the core cross-section, is shown in Figure 4b. The outer diameter of the core is greater by 0.1 mm than expected due to the interpenetration of the strip and the rolls. As a result of rolling, a bimetallic bar elongation by a factor of 3.5 was achieved. The displacement of metal through the whole roll gap takes place during approx. 6 rotations, which causes a reduction of the bar radius by 0.6 mm per single roll action.

3.1. Analysis of rolls diameters influence on the rolling process

On the basis of numerical modelling performed according to Variants I and II it was possible to determine the effect of roll diameter on the course of the process, as well as on the distribution of stress and strain and rolling power.

Figure 5a shows schematically the area of contact with the rolls during rolling on rolls with diameters of 60 mm and 100 mm, respectively. The area of contact of the sample with 100 mm-diameter rolls is much greater than in the case, where rolls of a smaller diameter are used. The computer simulation results indicate a considerable increase in rolling power in Variant II. When analyzing the data in Figure 5b it can be found that the rolling power is dependent on the roll contact area. A larger contact area involves larger overall roll separating forces, which has an effect on the rolling power.

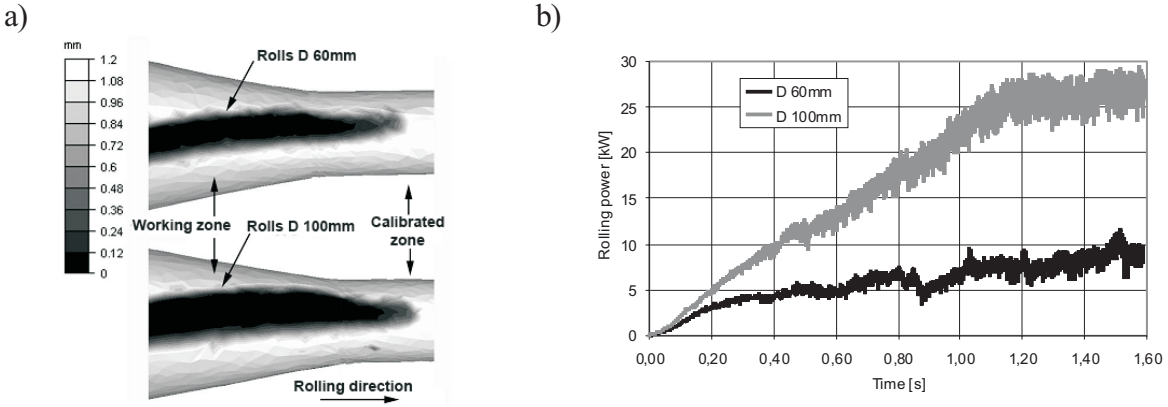

Fig. 5. Results of numerical modeling: a) contact area between sample and rolls, b) distribution of rolling power for two roll diameters

On the other hand, however, the process of rolling according to Variant II is more stable owing to the roll bite conditions. The occurring roll slip, particularly in the initial phase of rolling, is lesser than for rolling according to Variant I. It should be noted, however, that the roll diameter is dependent on the diameter of bar being rolled and, due to the geometrical conditions, it may not be too large.

An analysis of the distribution of stress and strain intensities was performed within the work. Figure 6 shows the distributions of stress effective on the sample cross-section for Variants I and II. The cross-sections are made: in the plane of deformation zone entry, in the mid-length of the roll gap, and in the plane of sample exit from the rolls working part.

The stress effective distributions shown in Figure 6a (Variant I) have higher values compared to the stress effective distributions shown in Figure 6b (Variant II). The increased stress effective values (approx. 250 MPa) in Variant I of rolling occur locally, in the vicinity of the roll contact locations. Effective values in Variant II are lower (approx. 210 MPa).

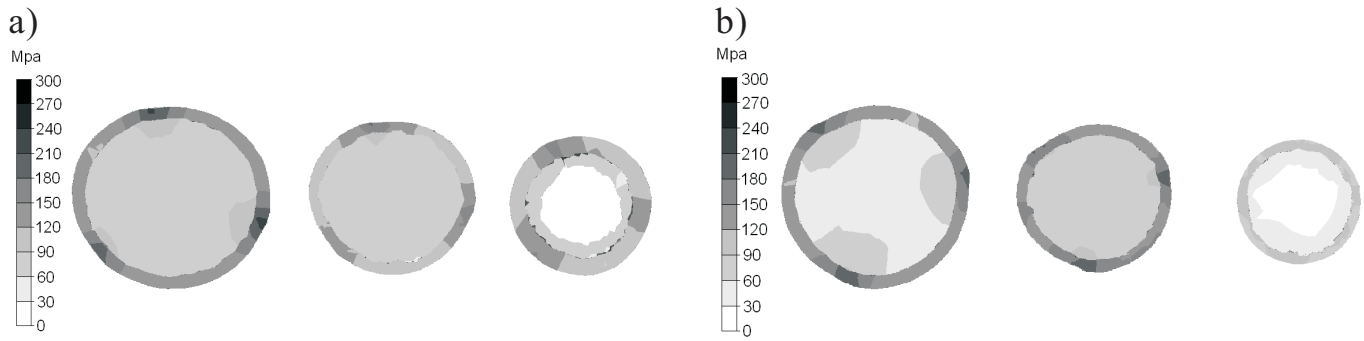

Fig. 6. Distribution of stress effective on the sample cross-section: a) roll diameter 60 mm, b) roll diameter 100 mm

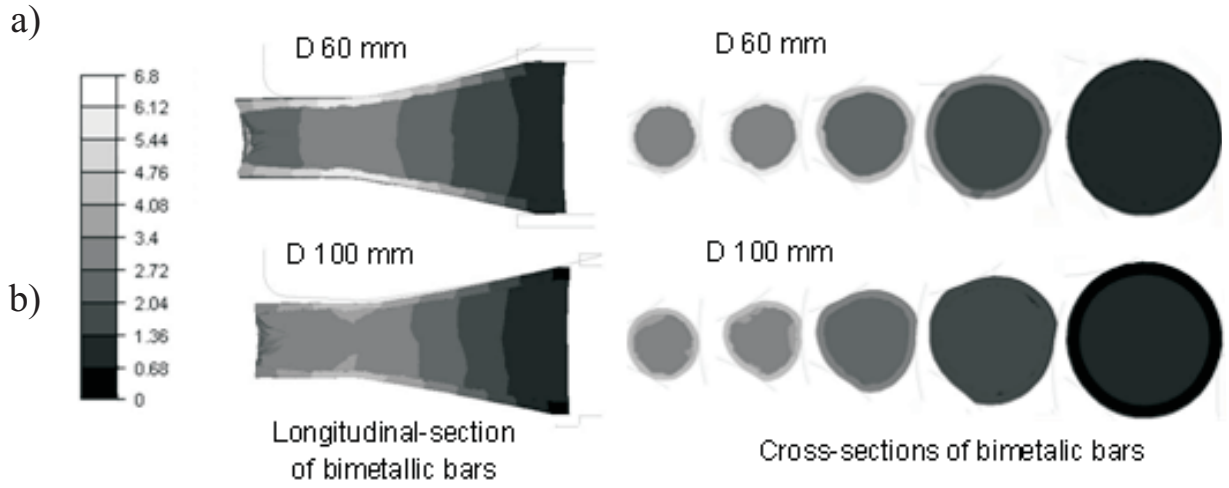

Fig. 7. Distribution of strain effective on the sample cross-section and sample longitudinal-section: a) roll diameter 60 mm, b) roll diameter 100 mm

When analyzing the strain effective distributions for Variants I and II of rolling (Fig. 7) it can be found that the deformation of sample according to Variant II progresses more "smoothly", and the distribution of strain effective over the length of the deformation zone has a more uniform behaviour (Fig. 7b). In the case of rolling with the use of a smaller roll diameter (Variant I), the strain effective distribution is less uniform. In this variant, the strain effective magnitudes are greater (approximately 6) and occur in the vicinity of the roll working part.

3.2. Analysis of rolls rotational speed influence on the rolling process

An analysis of the effect of roll rotational speed on the stability of the rolling process and the strain and stress distributions was carried out in this work. Two rolling variants were analyzed: Variant I, in which roll

rotational speed was 100 rpm, and Variant III with a roll rotational speed of 200 rpm. From simulations carried out it was found that the process of rolling in Variant I ran stably, with a small roll slip – the whole bimetallic feedstock length was rolled out to produce a final diameter of 20 mm. In Variant III, the process ran unstably and roll slip took place, which caused the termination of the rolling process. Figure 8 shows the distribution of the component of the velocity of bimetallic feedstock flow in the rolling direction for both variants analyzed.

Comparison of both variants shows that the process of rolling according to Variant I ran without the involvement of the centring tool (i.e., the centring tool did not press down on the feedstock), as shown in Figure 8a. In Variant III, in the initial phase of rolling, the process progresses without the involvement of the centring tool. As the feedstock is moved into the roll gap, the deformation resistance increases, which results in a stop of the deformed sample in the mid-part of the roll gap and a roll slip (Fig. 8b).

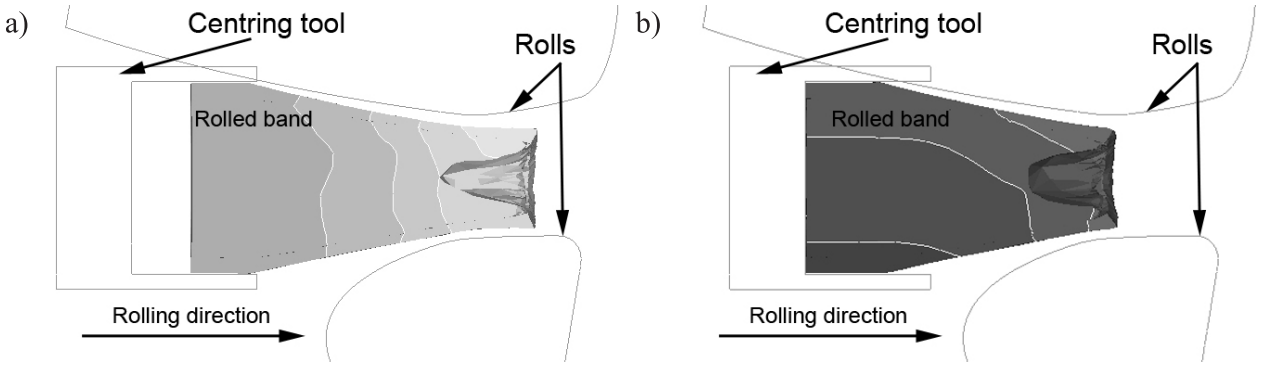

Fig. 8. Distribution of velocity metal flow in the rolling direction on the sample longitudinal-section: a) rotational speed 100 rpm I, b) rotational speed 200 rpm

The sample remains for some time at the same place in the roll gap, until the centring tool starts pressing the strip down. In the initial phase of rolling, an intensive effect of surface layers "flowing down" is observed on the strip end face. As a consequence, a void forms within the bimetallic strip Fig. 8). Increasing deformation resistance and the occurrence of a slip promote also the occurrence of the strip triangulation effect, which in extreme cases makes further rolling impossible.

The cause of a roll slip and a strip stop is an increased roll rotational speed. Increasing roll rotational speed from 100 rpm to 200 rpm (with the remaining process parameters unchanged) causes an increase in strain rate in the strip being rolled from 12 s^{-1} to 20 s^{-1}. Such an increase in strain rate substantially increases the stress, especially at such large deformations, as those applied in rolling on the three-skew rolling mill (i.e. from 40 to 50%). The increase in the magnitude of stress causes an increase in deformation resistance and, as a consequence, a roll slip.

An analysis of the distribution of stress and strain effective was performed within this work. Figure 9 shows examples of stress and strain effective distributions on the cross-sections of sample being rolled, made in the mid-length of the roll gap.

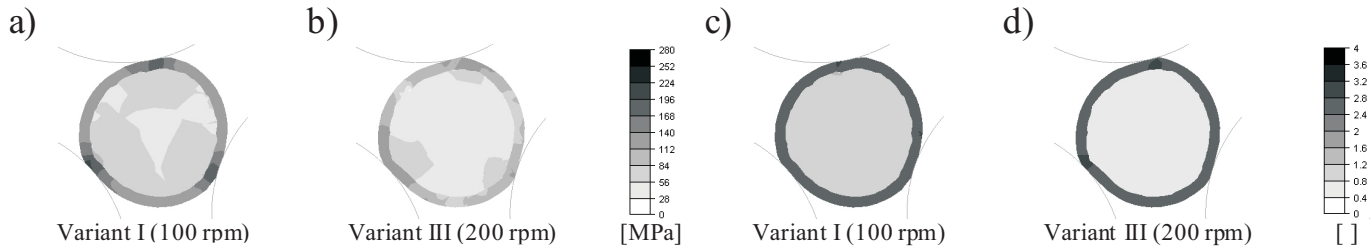

Fig. 9. Distribution of rolling parameters on the sample cross-section: a,b) stress effective, c,d) strain effective

The stress and strain analysis is difficult because of a slip during rolling occurs. The values of stress effective during rolling in Variant I (Fig. 9a) are greater by approximately 25 MPa compared to Variant III (Fig. 9b). Higher values of strain effective are also observed in Variant I (Fig. 9c, 9d). The lower values of stress and strain effective in Variant III are indicative of the occurrence of a slip caused by unfavourable deformation conditions in Variant III. In the locations of contact between the rolls and the strip, locally occurs a higher strain effective magnitude.

A parameter that well characterizes the course of the rolling process is the rolling power. The variation of rolling power for Variants I and III is shown in Figure 10. When analyzing the graphs in Figure 10 it can be found that during rolling at a lower speed (100 rpm) the process ran stably with a small roll slip, as evidenced by the small local power increases.

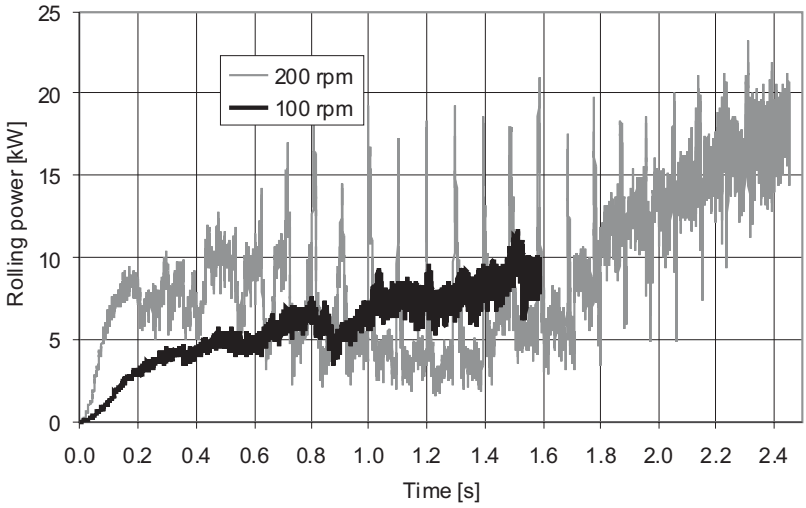

Fig. 10. Distributions of rolling power for rotational speeds: 100 rpm and 200 rpm

During rolling at a higher speed (200 rpm), large instantaneous power increments occur, followed by declines. This indicates that the process ran unstably, that is a pushing of the sample out of the roll gap took place. The rolling power increase after 2 seconds (for the speed of 200 rpm) is associated with the rolling stage, at which the centring tool pushes the material into the deformation zone. By comparing the results of studies on the process of rolling at rotational speeds of 100 rpm and 200 rpm it can be concluded that the deformation conditions are more favourable when rolling at a lower speed.

4. Conclusions

Theoretical tests carried out have demonstrated that the application of a larger roll diameter has a favourable effect on the rolling process. The rolling progresses more stably, and a smaller slip occurs between the rolls and the strip being rolled. When using rolls with a smaller diameter, a greater slip occurs; the power demand is, however, lower. Further studies will make it possible to optimize the roll diameter so that the process runs stably with a lower power demand.

On the basis of the performed numerical studies of the process of rolling on the three-skew rolling mill it can be stated that the rolling speed considerably influences the stability of the process being run.

The deformation conditions prevailing in the deformation zone are more favourable during rolling at a roll rotational speed of 100 rpm. At a rotational speed of 200 rpm, a roll slip was observed, which prevented the correct run of the rolling process.

Researches was made within a framework to Developmental Project No. R07 022 02 financed by Polish Ministry of Sciences and Higher Educations.

REFERENCES

[1] T. Kahrs Jason, Darwin David, E. Locke Jr. Carl, Evaluation of corrosion resistance of type 304 stainless steel clad reinforcing bars, A Report on Research Sponsored by The National Science Foundation, Research Grant No. CMS – 9812716, The University Of Kansas Center For Research, August 2001.

[2] K. Nakasuji, K. Maruda, C. Hayashi, Development of Manufacturing Process of Clad Bar by Rotary Rolling, ISIJ International **37**, 9, 899-905 (1997).

[3] H. D y j a, S. M r ó z, D. R y d z, Technologia i modelowanie procesów walcowania wyrobów bimetalowych. Wydawnictwo WIPMiFS Politechniki Częstochowskiej 2003, Seria Metalurgia No. 33.
[4] S. M r ó z, Teoretyczno – doświadczalna analiza procesu walcowania bimetalowych prętów, Praca doktorska, Politechnika Częstochowska 2002.
[5] S. P. G a l k i n, H. D y j a, A. M. G a l k i n, A. R z ą s o w s k a, Kinematyczny model płynięcia metalu podczas walcowania skośnego prętów, Hutnik, Wiadomości Hutnicze, No. 12 (74), 2004 r.
[6] FORGE3® Reference Guide Release 6.2, Sophia-Antipolis, (2002).

Received: 20 May 2009.